

Design Optimization of a Multi-material, Fiber-reinforced Composite-intensive Body-In-White of a Mid-Size SUV

Amit M. Deshpande^{1,2}, Rushabh Sadiwala³, Nathan Brown³, Pierre-Yves Lavertu^{1,4}, Sai Aditya Pradeep^{5,6}, Leon M. Headings⁷, Ningxiner Zhao⁷, Brad Losey⁷, Ryan Hahnen⁸, Marcelo J. Dapino⁷, Gang Li³, Srikanth Pilla^{1,2,4,9*}

¹Center for Composite Materials, University of Delaware, Newark, DE 19716

²Department of Mechanical Engineering, University of Delaware, Newark, DE 19716

³Department of Mechanical Engineering, Clemson University, Clemson, SC 29634

⁴Department of Materials Science and Engineering, University of Delaware, Newark, DE 19716

⁵Clemson Composites Center, Clemson University, Greenville, SC 29607

⁶Department of Automotive Engineering, Clemson University, Greenville, SC 29607

⁷Department of Mechanical & Aerospace Engineering, The Ohio State University, Columbus, OH 43210

⁸Strategic Research Operations, Honda Development & Manufacturing of America, LLC

⁹Department of Chemical and Biomolecular Engineering, University of Delaware, Newark, DE 19716

1. ABSTRACT

Transportation accounts for almost a third of all energy consumption and emissions in the U.S. With an emphasis on improving the energy efficiency of vehicles and transitioning to electrified vehicles, lightweighting has become relevant to compensate for the added complexity of battery packs and hybrid powertrains. Lightweight materials such as aluminum, magnesium, and fiber-reinforced plastic (FRP) composites can reduce the vehicle's structural mass, the body-in-white (BIW), by up to 50%. However, the higher proportion of large sports utility vehicles (SUVs) and trucks in the North American fleet poses a challenge, as the larger size and high production scale of the structural components for this segment can significantly increase material costs. Thus, a multi-material approach to deploy FRP composites at select locations in an existing metal BIW can help advance composites design, integration, and manufacturing technologies. Furthermore, these designs can be translated for future EV structures.

This study utilizes a systems approach to 1) establish design targets through structural analysis of the baseline SUV BIW design under various static and dynamic load cases, 2) conceptualize multi-material designs, and 3) assess the designs to meet lightweighting, cost, and sustainability objectives. Sustainable recycled carbon fiber-reinforced composites and other cost-effective FRP composite materials manufactured using state-of-the-art high-pressure resin transfer molding (HP RTM) technology were assessed for use in structural elements. An ultrasonic additive manufacturing (UAM) technique was implemented to produce mechanically interlocked metal-fiber transition joints to serve as a joining mechanism between fibers and metals in the multi-material design. To incorporate the transition joint design into the topology optimization scheme, a high-fidelity model of the fiber-metal transition joints that describes the fiber-oriented interactions between the fibers, cured-epoxy matrix, and metal components was developed. This model's results accurately represented the behavior from experimental testing. They can be transferred to the FEA solver as a computationally efficient material card specifically for use at the metal-composite transition regions in the proposed designs. The results from this system-level multi-material composites integration study have been presented.

*Keywords: carbon fiber, lightweighting, multi-material joining, optimization

*Corresponding author: spilla@udel.edu ; Ph: [302-831-8149](tel:302-831-8149)

2. INTRODUCTION

Lightweighting has been the focus of research and development efforts for automakers since the 1970s. Following the introduction of CAFE standards as a legislative response to the oil crisis, lightweighting gained impetus, with plastics and composites emerging as prominent material systems for non-structural and semi-structural applications [1]. Unreinforced plastics became commonplace for interior and exterior trim of the vehicles, while discontinuous short- and long-fiber reinforced plastics (FRPs) were used for semi-structural applications. They, however, lacked the mechanical performance in terms of stiffness, strength, and impact resistance required for use in automotive structural applications [2] such as the closures of the vehicle, exterior structural panels such as the roof and the primary structure, i.e., the body-in-white (BIW). Thus, continuous fiber-reinforced composites have become the focus of research efforts to enable lightweight structural automotive components, reinvigorating the use of plastics in automotive vehicles, as summarized in Figure 1.

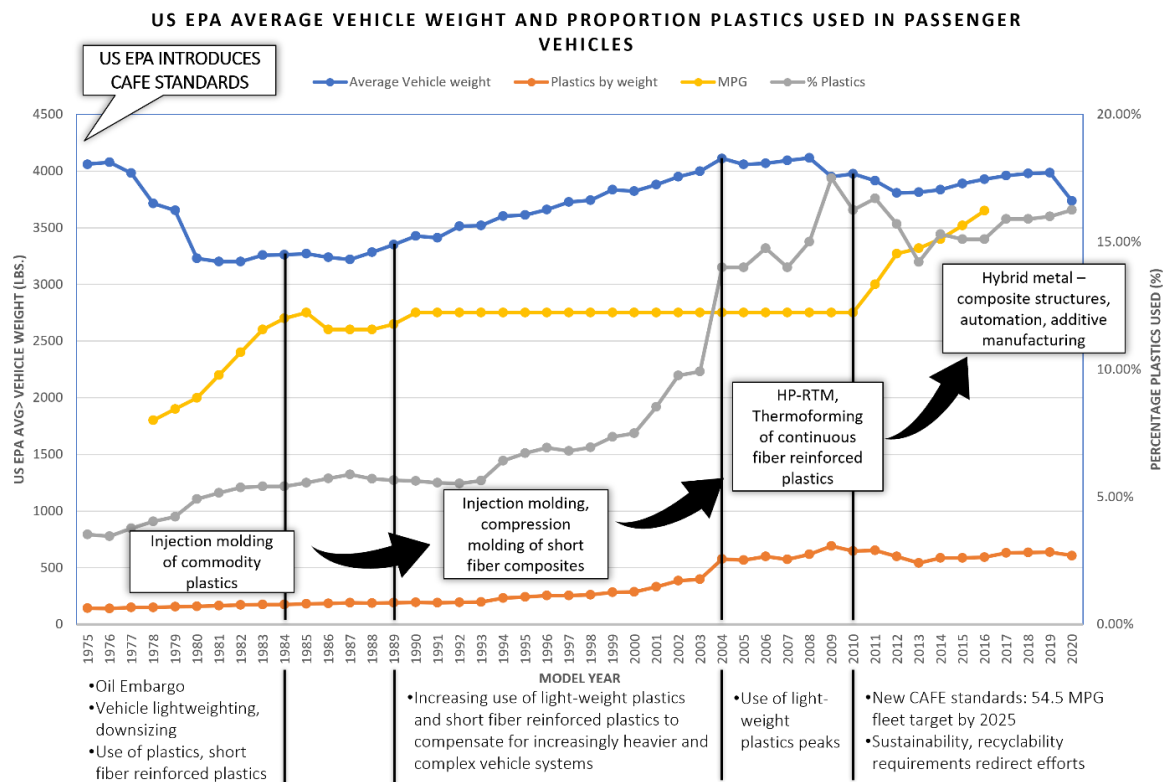


Figure 1: US Regulations driving impetus for use of plastics [3][4][5]

Continuous carbon fiber reinforced composites also have the highest weight reduction potential among all commercially available lightweighting material technologies, such as advanced high-strength steels, aluminum, magnesium, and titanium, while being less susceptible to corrosion and more energy efficient in manufacturing [6]. However, the high cost of continuous fibers, especially carbon fiber, and their preforms inhibit automotive adoption. As the scale of production increases, the material cost becomes the dominant cost for any vehicle component, especially for large structural components[6], limiting continuous fiber-reinforced composites to luxury and sports vehicles. Thus, a multi-material design approach is more feasible, with metals and FRPs used

selectively in certain locations in a mutually beneficial manner to achieve cost-effective lightweighting as illustrated in Figure 2.

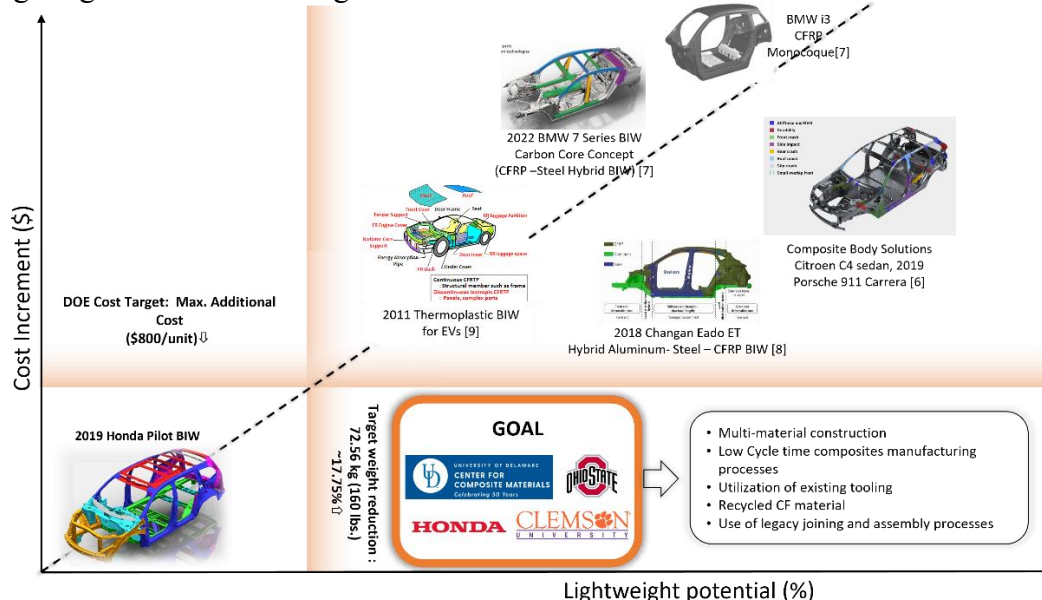


Figure 2: Cost v/s Lightweighting potential trade-offs for different multi-material lightweight designs for BIWs [7] [8] [9] [10] [11]

However, the joining of FRP composites with metals has its challenges. It is difficult to achieve a metallurgical bond between FRP composites and metals with conventional welding processes, while mechanical fastening increases assembly complexity. It leads to high-stress concentration regions, reducing the structure's strength, stiffness, and toughness. Adhesives are a promising option being adopted by OEMs to join aluminum with hard and brittle advanced high-strength steels (AHSS) and ultra-high-strength steels (UHSS) [12] among other lightweight structural materials. However, the need to have sufficient contact area for the adhesive to be effective, meticulous preparation of bonding surfaces, the brittle nature of adhesives (especially epoxies) [13] as illustrated in Figure 3, and the added adhesive and flange weight are inhibiting factors. Hybrid joining methods provide a potential solution where the mechanical interlocking between metal and composite is molded into the component during the liquid composite molding process [14] without leading to stress concentration.

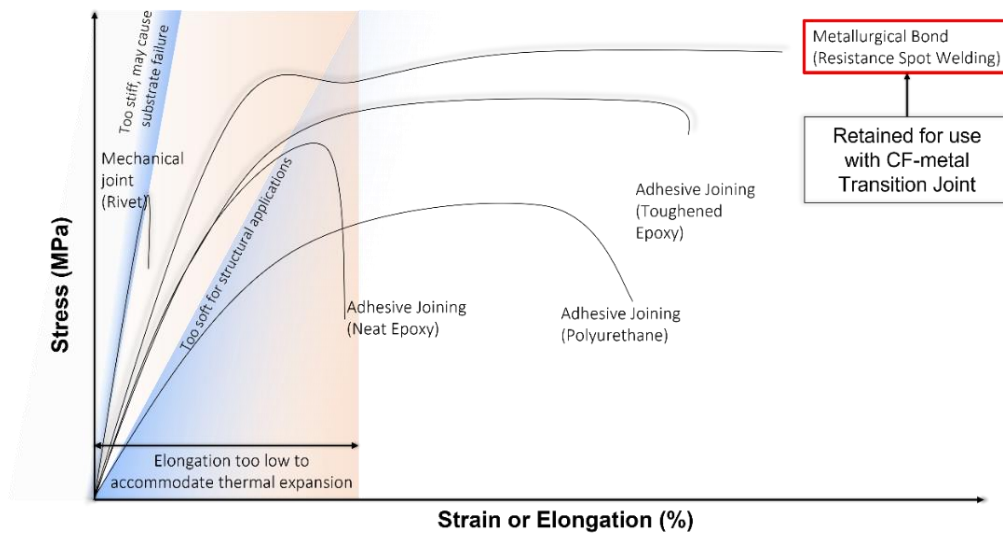


Figure 3: Normalized stiffness, elongation, and toughness - adhesives v/s metallurgical welding [13]

One such proposed methodology for multi-material joining is to leverage low-temperature ultrasonic additive manufacturing (UAM) of metal foils to build metal tabs around continuous fiber loops at the end of woven continuous fiber preforms. The preforms are then infused with resin, resulting in an FRP component with metal tabs at locations where it can be welded to the surrounding vehicle structure, as illustrated in Figure 4.

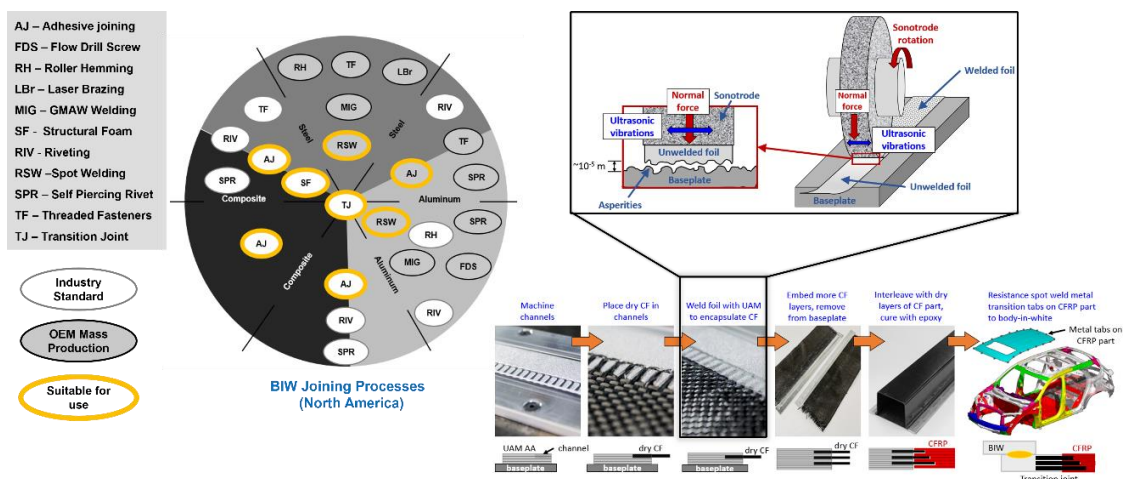


Figure 4: (left) Selection of OEM compatible processes for multi-material joining; (right) workflow for using UAM to fabricate composite parts with metal tabs [6]

Traditional composite manufacturing processes such as vacuum infusion, automated fiber placement (AFP), and in-autoclave prepreg molding cannot achieve the low cycle times required for automotive components without increasing the number of manufacturing lines. Thus, out-of-autoclave (OOA) liquid composite molding (LCM) processes such as high-pressure resin transfer molding (HPRTM) [15], wet compression molding (WCM), and dynamic fluid compression molding (DFCM) [16] have become the focus of development efforts. Furthermore, thermoplastic forming [17], [18], and injection over-molding have been proven to be cost-effective manufacturing methods for continuous fiber-reinforced components at cycle times desired by the automotive industry [19]. These processes are suited to fabricating complex components with

shell-like topology, representing the bulk of stamped sheet metal components comprising the unibody BIW architecture, as illustrated in Figure 5.

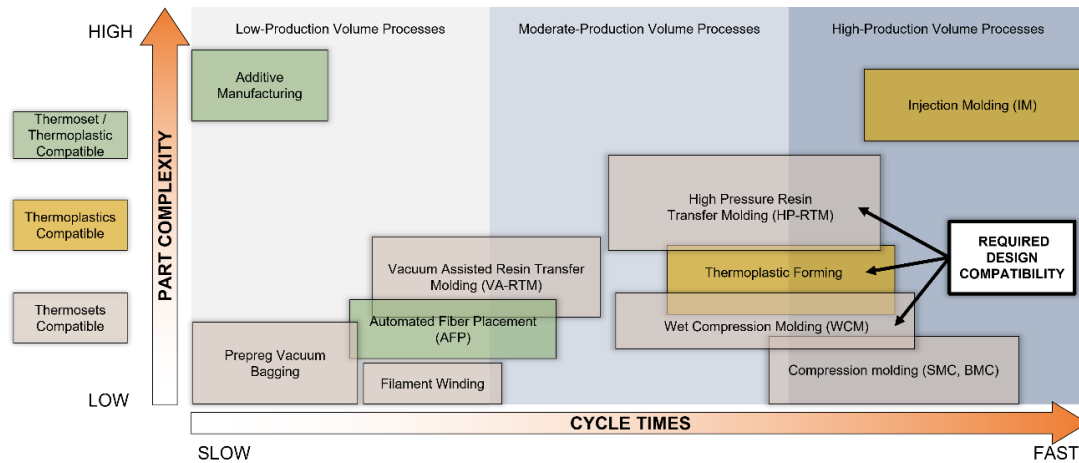


Figure 5: Manufacturability v/s cycle time comparison of composites manufacturing processes

3. SYSTEMS ENGINEERING APPROACH

With the above material, manufacturing, and joining considerations, the key technical challenges that remain are the development of optimized multi-material designs for the BIW components, the development of a system for assessment of lightweighting achieved, parts consolidation achieved, manufacturing costs, and identifying the right trade-offs. Furthermore, the design development approach must evaluate all possible concepts and design iterations before a design or optimization decision is taken. Thus, a systems approach was taken to establish quantified structural performance requirements based on structural analysis under static and dynamic load cases for the baseline steel BIW. Static load cases were simulated on Altair Hyperworks using the Optistruct solver as a linear static elasticity problem in conjunction with the inertia relief method. A decision matrix was established with criteria derived from high-level program objectives of lightweighting, cost, manufacturing throughput per year, and compatibility with OEMs existing joining and assembly infrastructure. Based on the structural analysis results of the baseline steel BIW, a requirements map was generated for various regions of the BIW based on desired material properties, namely stiffness (Young's Modulus), ductility (high elongation before failure), and strength (Ultimate Tensile Strength). Based on this requirements map, assemblies were identified for the potential use of FRP composites.

Designs leveraging various lightweight materials like glass fiber reinforced plastic (GFRP) and carbon fiber reinforced plastic (CFRP) composites, aluminum, HSS and AHSS were proposed for various assemblies comprising the BIW, resulting in multiple designs for each of the regions of the BIW. These assembly designs were combined into five unique BIW conceptual designs which were assessed for lightweighting, and parts consolidation potential using simple parametric models. Feedback from the OEM was used to grade each BIW conceptual design. These three metrics helped down-select the two most promising BIW conceptual designs for further finite element analysis (FEA) and optimization studies [6] as illustrated in Figure 6. CFRP and GFRP composites were used at locations requiring high stiffness and moderate-to-high strength.

However, regions that require high ductility and high strength, implying high toughness, have been retained to be made from baseline steel.

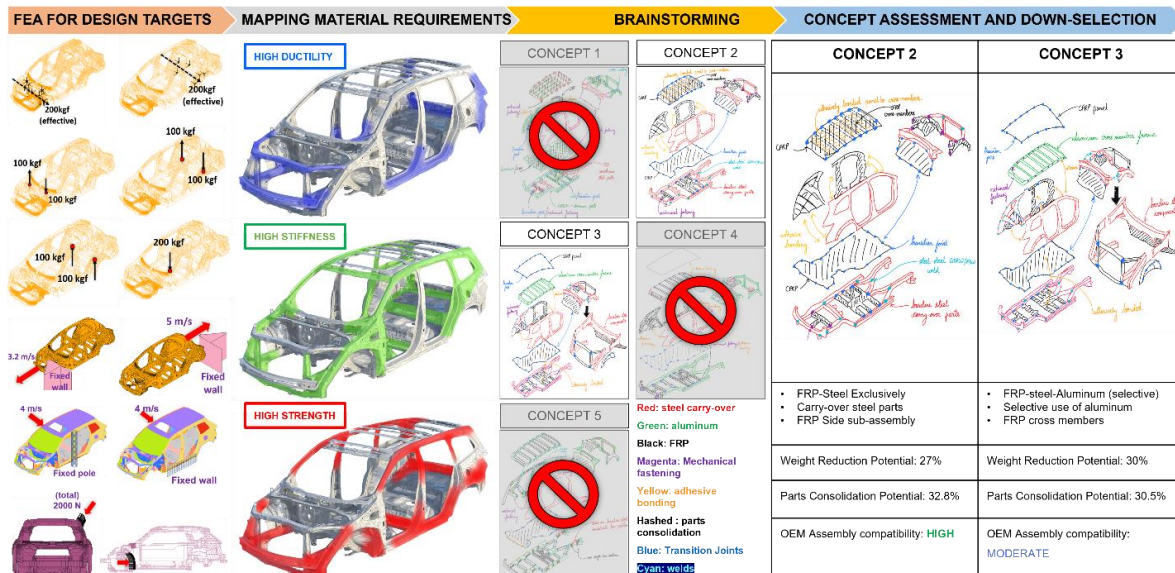


Figure 6: Systems approach to design conceptualization and down-selection [6]

4. DESIGN DEVELOPMENT

4.1 Concept 1 – Composite Roof and Sub-Frame assembly

The first BIW conceptual design focused on simplifying the design of the roof assembly, the floor assembly, and the sub-frame assembly using composites, as illustrated in Figure 7. Part consolidation and design simplification were heavily leveraged to ensure cost parity with the baseline steel designs being replaced. The baseline roof assembly consists of the panel made of 0.7 mm thick bake hardenable steel and eight cross members made from cold rolled steel varieties with thicknesses ranging from 0.7 mm to 1.2 mm. Excluding the front and the rear cross members, all other members were either eliminated or redesigned to be fabricated out of CFRP using the HPRTM process, owing to their slightly complex geometry. The roof panel was proposed to be fabricated from a hybrid ply stack-up of carbon fiber and glass fiber reinforced composites using the WCM process, owing to the simple almost-flat panel geometry.

The mid-rail and rocker beams' baseline material and design were retained for the sub-frame assembly. In contrast, the cross members and central members between the A-pillar and C-pillar of the sub-frame were consolidated into a single CFRP-GFRP hybrid composite component, with the design complexity suitable for manufacturing using HPRTM. The floor panel, made from 0.65 mm thick dual-phase steel, was redesigned to be fabricated from GFRP composites using the WCM process, owing to its simple flat-panel geometry. Adhesive bonding and UAM transition joints, suitable for resistance spot welding, were the two joining methods proposed for use when joining the composite components to the surrounding baseline steel components. Adhesive bonding has been extensively investigated and demonstrated for use (as detailed in section 2), while the transition joint has been demonstrated to be a feasible joining method by Honda [20]. These designs were evaluated for structural performance to validate the concept and ensure the design was being developed and refined in the right direction. The designs were developed as surfaces, and the minimum thicknesses for the composite components to meet the baseline

performance targets of allowable deformation (global stiffness) without failure (maximum stresses below the yield strength of the as-manufactured composite laminate) were determined iteratively.

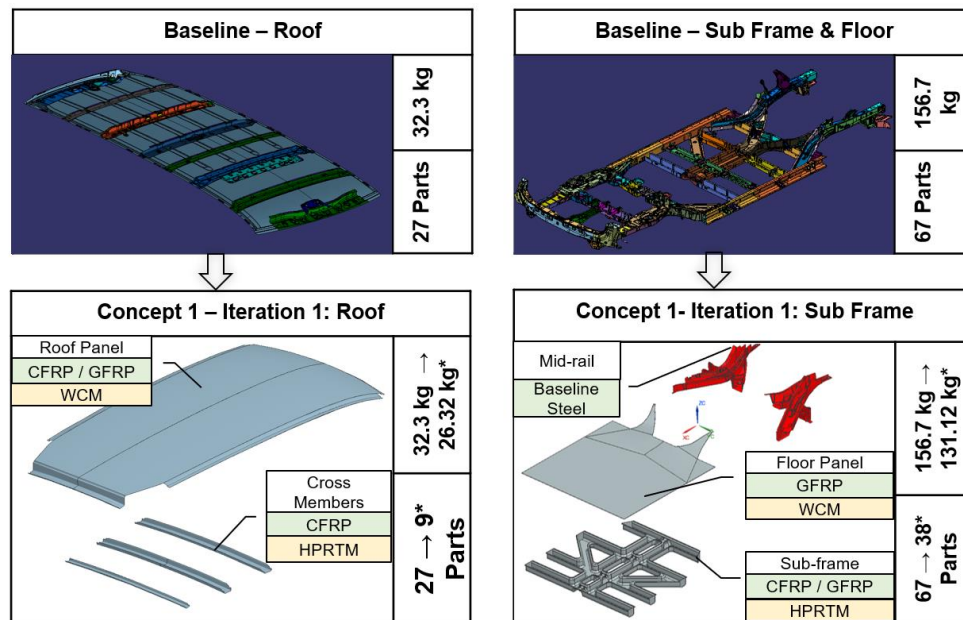


Figure 7: Redesigned roof and sub-frame assemblies using continuous fiber reinforced composites.

4.2 Concept 2 – Composite Side Frame Assembly

This concept focused on the side frame with the complex assembly redesigned into five distinct CFRP components on each vehicle side. As illustrated in Figure 8, the side frame has the highest potential for parts consolidation. Thus, 10 composite parts would replace 110 baseline steel components to significantly reduce the costs associated with multiple sheet metal stamping tools and cycle time savings due to reduced joining and assembly steps while ensuring significant lightweighting. Furthermore, material costs are expected to reduce further as optimization of the composite laminate at the ply stack-up and ply shape level is implemented, and expensive carbon fiber is optimized.

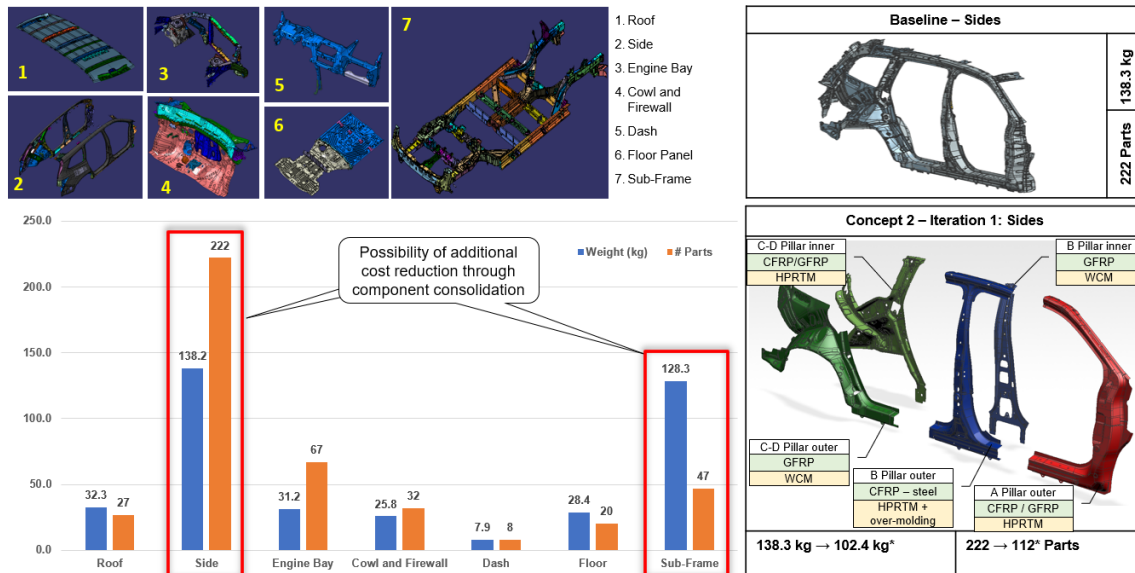


Figure 8: (left) BIW assemblies' breakdown, (right) Redesigned side-frame assembly using continuous fiber-reinforced composites.

5. DESIGN ASSESSMENT

5.1 Structural Performance Assessment -FEA

Both design concepts are analyzed under the same load cases as the baseline model. The load cases were established after a discussion with the OEM and are shown in Figure 6. The composite parts are assumed to be 4mm thick with 4 plies in a $[0,45,-45,90]^\circ$ orientation. Each ply is a 1mm thick uni-directional CFRP fabricated using Westlake Epikote snap-cure epoxy. (MAT8 material card on Altair Optistruct, MAT58 material card on LS-Dyna). As this initial analysis is done to test the viability of the concepts, the thicknesses chosen are the upper limit of final thicknesses. Hence, the weight reduction achieved leaves significant room for improvement. The composite parts are assumed to be connected via spot connections at the same points as the baseline model. The static load cases are simulated on Altair Optistruct using linear static analysis. The stiffnesses for static load cases are defined as the average ratio of applied forces to the resultant displacement at the same points. The dynamic load cases are simulated on LS-Dyna using a linear material, large deformation explicit dynamic formulation. As we are only interested in the stiffnesses, this analysis is sufficient. In the future, a full elastoplastic crash analysis will be performed. The linear explicit analysis terminates at $t=10\text{ms}$. The stiffnesses for dynamic cases are defined as the initial slope of the force-displacement curve. For each load case, the extracted stiffnesses are compared to the baseline and documented in Figure 10(a).

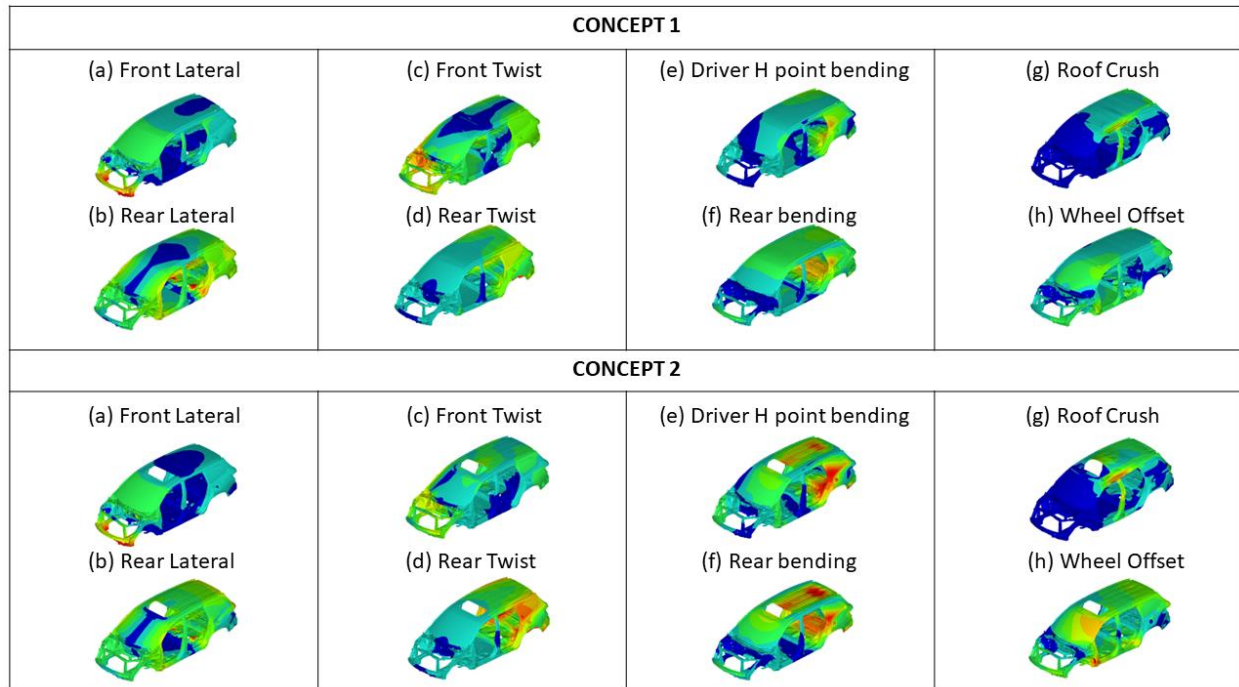


Figure 9: Displacement plots – Static structural analysis of 1st Iteration of the two design concepts

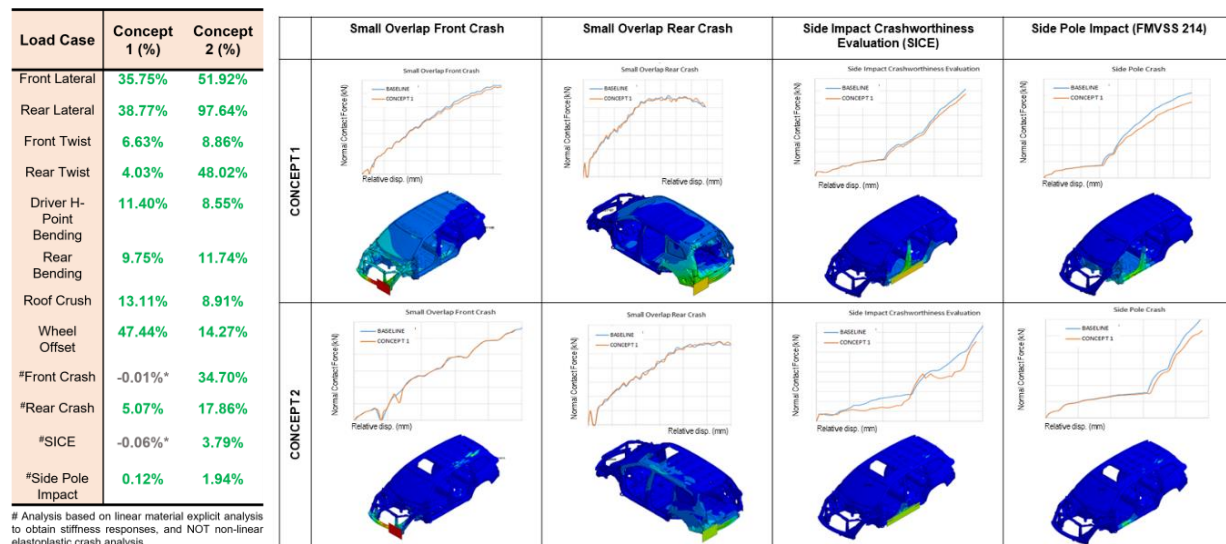


Figure 10: (a) Stiffness of the design concepts compared to baseline (b) Dynamic (linear) structural analysis – Force vs displacement and displacement contour plots.

5.2 Cost modeling

Once the proposed design concepts were verified to meet structural performance requirements within acceptable limits, the cost was assessed using a parametric cost model. The model factored in material, manufacturing, machine, tooling, and overhead costs with reasonable assumptions, as illustrated in Figure 11. Each proposed composite part was assessed using this model, and the weight reduction achieved was used to calculate the cost increase per pound of weight reduced. This metric was then compared with the project objective of a maximum of \$5 increase per pound

reduced[6] to determine if the proposed designs aligned with the cost objectives. The inputs to this cost model and the underlying assumptions have been summarized in Table 1.

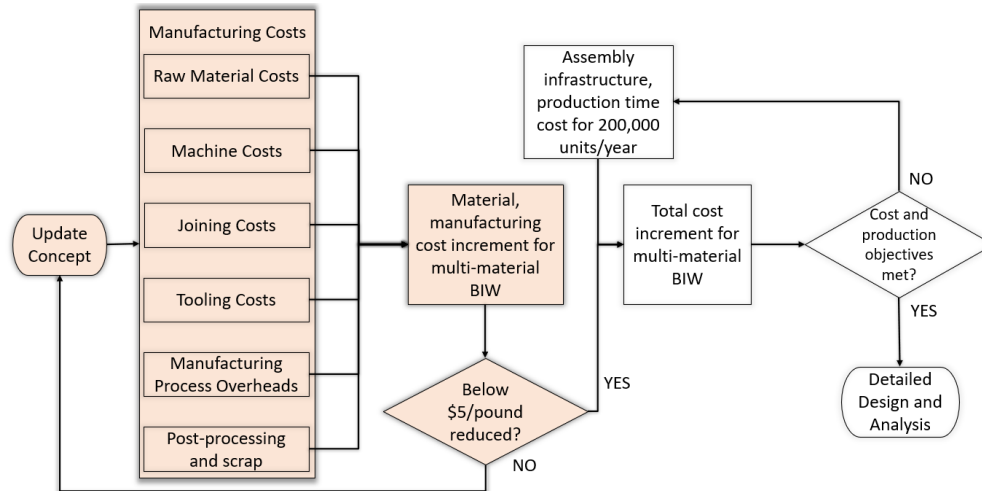


Figure 11: Factors considered in the development of the parametric cost model (highlighted steps investigated)

Table 1: Parametric Cost Model Assumptions, Inputs.

Assumptions		Manufacturing Cost Inputs	
Composite Part Thickness	4 mm	Carbon Fiber - Epoxy Cost[19]	\$15.54 /kg
HPRTM Cycle Time	6 min/part	HPRTM equipment cost [19]	\$7,293,000
WCM Cycle Time	6 min/part	WCM equipment cost [19]	\$817,300
Equipment Life	20 years	Power rating for HPRTM	260.74 kW
Tool Life	1,000,000 cycles	Power rating for WCM	176.43 kW
Labor cost	\$15/hour	Transition joint fabrication cost	\$1.15/m
Material scrap rate	4 %	P20 tool steel (C_{steel})	\$11.48 / kg
Energy costs	\$0.075/kWh		
Overhead costs	15 %		
Part Rejection rate (6 σ standard)	3.4 parts / million		

The CF-metal transition joint fabrication cost is calculated considering the cost of woven carbon fiber and cost of aluminum 6061. This resulted in a higher cost for a transition joint that utilized a less expensive glass fiber or a cheaper metal like mild steel, allowing for a conservative cost estimate, as shown in

Table 2. The mass ratio of the parts replaced with composite designs to the total baseline mass was determined to calculate the cost of baseline sheet metal components replaced. This approach allows efficient estimation of cost v/s lightweighting feasibility without delving into the manufacturing costs of the baseline steel components. Thus, the cost of design changes is captured without directly comparing the detailed cost of the entire multi-material BIW concept with that of the baseline steel BIW. The cost of replaced components is summarized in Table 3.

Table 2: Material and Fabrication costs for CF-metal transition joint.

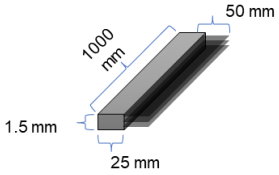
Joining Method	Cost per unit		\$/m	Comments	 <p>Figure 12: CF-metal transition joint geometry</p>
UAM CF-Al transition materials with epoxy	Woven CF: \$19.8 /kg (\$9.07/lb)	Al: \$4.4 / kg (\$2.0/lb)	\$1.15	Pricing for 1" wide transition flange with 3 layers of embedded CF fabric as illustrated in Figure 12.	

Table 3: Mass Ratio and cost determination for replaced baseline components.

Concept	Mass ratio	Est. Cost of replaced baseline parts
Concept 1 – roof and sub-frame	0.1182	\$224.58
Concept 2 – side assembly	0.1796	\$341.24

The tooling cost required to manufacture the composite components using HPRTM or WCM was determined by estimating the tool volume (V_t) using the proposed composite design geometry. Sufficient offsets to the dimensions of the tool were considered to obtain a realistic estimation of the tool size. This volume was used to determine the cost of the P20 tool steel (C_{steel}) block that would be machined out and the cost of machining the tool itself, as given in Equation (1). It was assumed that approximately 30% (or 0.3) of the material was machined during the tool machining process. The cost of CNC machining was determined using hourly rate calculation to be \$68.39/hour and has been elaborated in the appendix. Furthermore, it is assumed that the costs of assembly of the composite parts are the same as those of assembling the steel parts. This will be updated once the concepts are refined, and a plant layout is developed to meet the yearly production objective. The total costs and distribution of the two concepts based on this initial cost model are shown in Figure 13.

$$\text{Tool cost} = (2 V_t C_{steel}) + (2 V_t 0.3 C_{steel}) 68.39 \quad \text{Equation (1)}$$

Although assembly costs have not yet been included, both concepts exceed the project cost targets (\$5/lb of wt. reduction). Concept 1, focusing on the roof and sub-frame assembly redesign, significantly exceeds the cost margin, necessitating reevaluation of the design and material choices. It was concluded from the cost analysis that replacing the material system used for large components, such as the roof and floor panel, with expensive composite materials, without associated parts consolidation is ineffective. Thus, further design refinement of this concept is necessary and has been addressed in subsequent sections. Concept 2, focusing on the side assemblies, is significantly closer to the cost target and underscores the need for lightweighting and parts consolidation in tandem.

The cost distribution by factors also highlights the dominance of material costs for large-scale production of structural composite parts. Additional reduction in cost is achievable as the design progresses and structural optimization of the use of expensive carbon fiber is performed. This is expected to reduce the part thicknesses significantly and, thus, the overall material costs, which are the largest factor. Using less expensive GFRP and mixed GF and CF hybrid designs based on the stiffness and strength requirements can further reduce material costs.

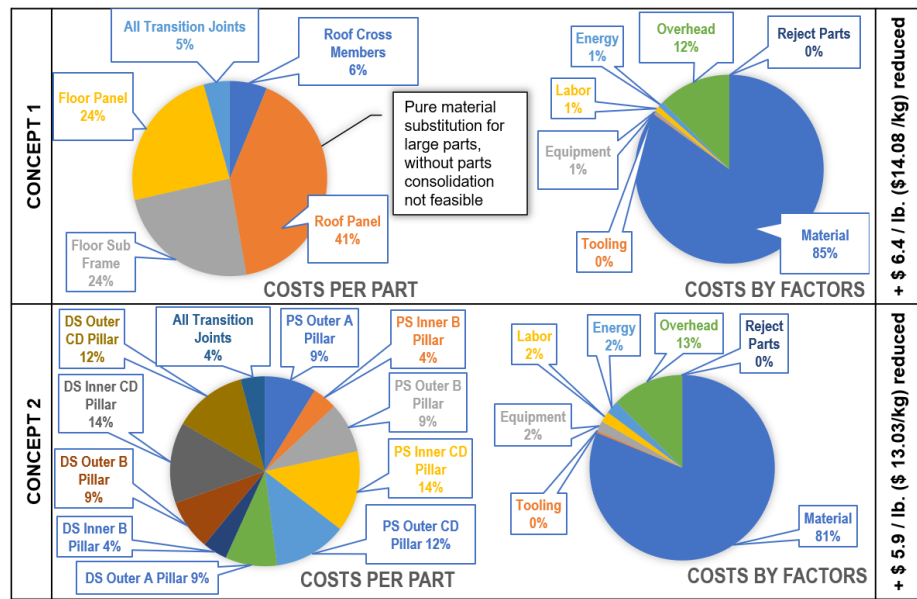


Figure 13: Initial cost analysis for iteration 1 of CAD concepts 1 and 2.

6. DESIGN REFINEMENT

6.1 Concept 1 – Composite Roof and Sub-Frame assembly (Iteration 2)

A key observation from the cost analysis was that it was not feasible to substitute lighter materials for some of the larger components, such as the roof panel and the floor panel, despite the geometries being less complex and easily manufacturable with WCM. The material cost was more dominant in such cases, making the designs infeasible. Thus, iteration two was formulated, wherein the major stiffening members are proposed to be made of composites. In contrast, the baseline designs and materials of the roof and floor panels are retained.

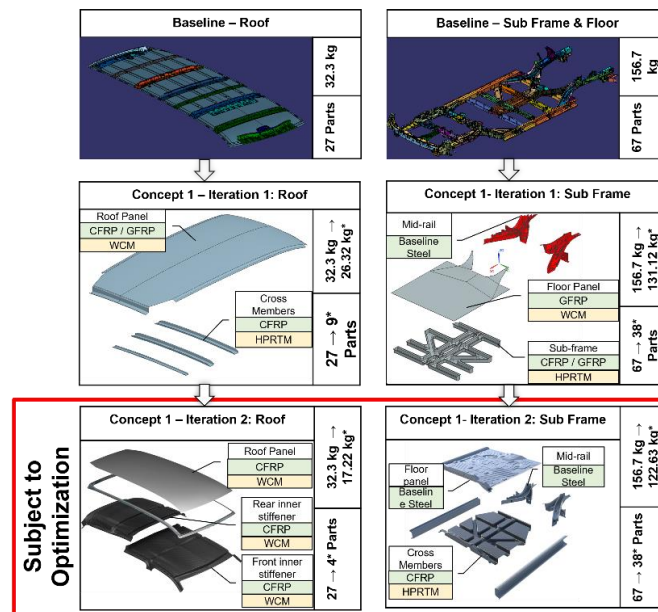


Figure 14: Redesigned roof and sub-frame using continuous fiber-reinforced composites – Iteration 2.

7. OPTIMIZATION

7.1 Optimization Methodology

Initially, the composite parts are assumed to be a 4-ply composite in a $[0,45,-45,90]^\circ$ orientation. The plies are assumed to be unidirectional CFRP plies. The number of plies and ply orientation are kept constant while optimizing the thicknesses (simple size orientation). In the future, as the designs are refined further, the optimization complexity will be increased to optimize both ply orientation (size optimization) and the number of plies (composite stack optimization). The optimization will happen in a two-step procedure. Initially, the ply thicknesses are kept free within the component and optimized. This results in a composite with varying thicknesses at different locations, similar to Topology Optimization (TO). However, unlike TO, it is not discrete. Based on these results, zones of uniform thicknesses will be defined in the composite part to reduce the manufacturing complexities.

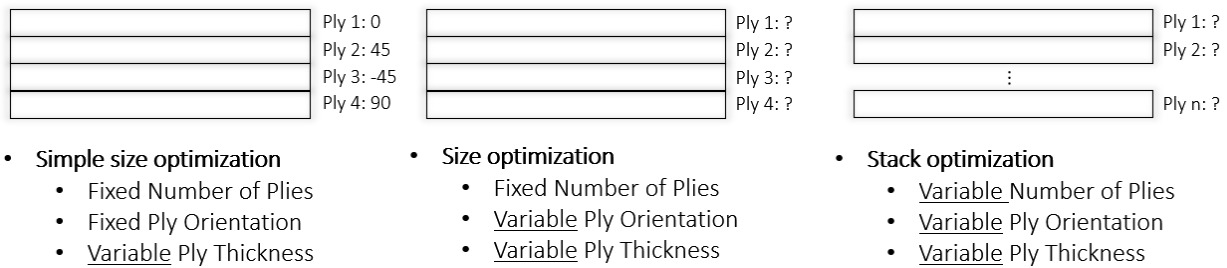


Figure 15 Composite optimization methodologies.

The optimization problem is formulated as:

$$\begin{aligned} &\text{Min } m \\ &\text{S.T. } K_i^c \geq K_i^b + sf \quad i \in 0,1, \dots n \end{aligned}$$

Where,

m is the total mass of the BiW

K_i^c is the stiffness of load case i , at the current iteration.

K_i^b is the stiffness of load case i for the baseline BIW.

sf is a safety factor, currently 5%

Currently, only static load cases are included in the optimization. Eventually, as the design is further refined, dynamic cases will also be considered. Finally, the designs will be optimized against full elastoplastic crash analysis.

7.2 Concept 1 -Iteration 2 Optimization Results

It can be observed in Figure 16 that the roof parts have a high thickness near the side rails of the frame. For their plies, it can be observed that high thickness zones of the 45-degree plies originate where the frame is attached to the B pillar of the BiW. The subframe thicknesses are more dispersed than the roof thicknesses. Based on these results, a zone can be established for the next optimization procedure. The total mass of the composite parts is reduced by 28.13 kg from the baseline, and the optimized concept meets all design requirements.

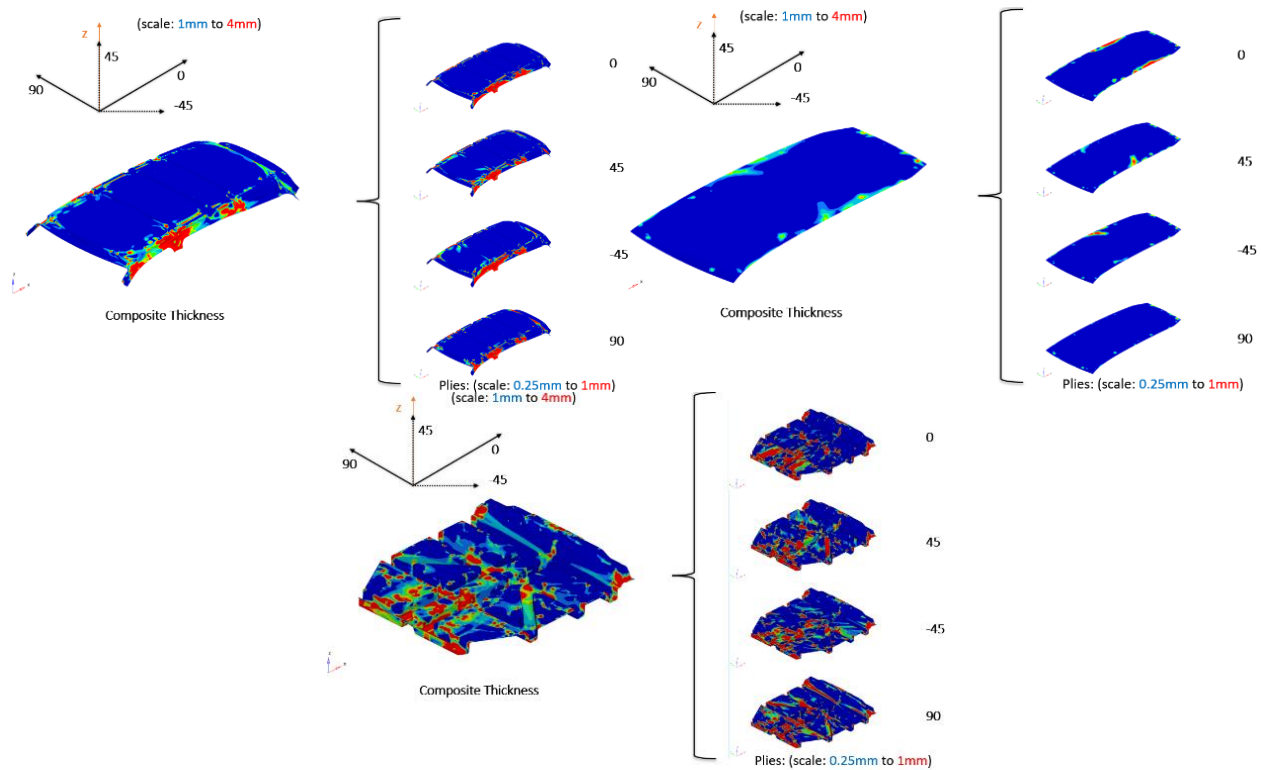


Figure 16: Optimized composite parts: (a) Front and rear roof frame (b) Roof Panel (c) Floor subframe.

Constraint	Concept 1 (%)
Front Lateral	0% (A)
Rear Lateral	0% (A)
Front Twist	7.16%
Rear Twist	2.02%
Driver H-Point Bending	8.64%
Rear Bending	4.75%
Roof Crush	1.58%
Wheel Offset	16.70%

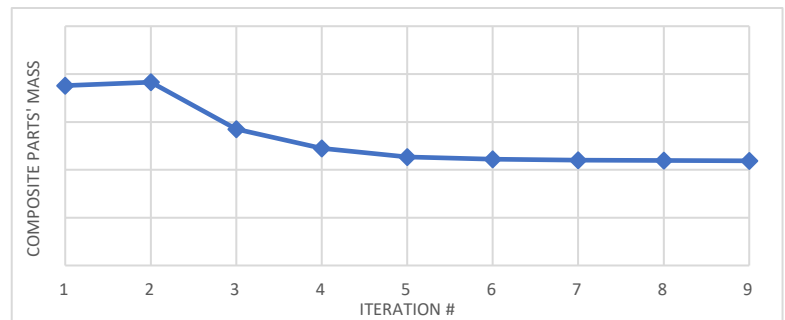


Figure 17 (a) Constraints at Convergence (b) Objective time history.

7.3 Optimized Design - Cost Assessment

The cost model is updated to reflect the optimized thicknesses for the concepts. All assumptions and parameters are the same, as explained in Section 5.2. The material cost and the cost targets are significantly lower than when the thicknesses were not optimized. The cost for the optimized model meets the project goal of a maximum of \$5/lb of weight reduced.

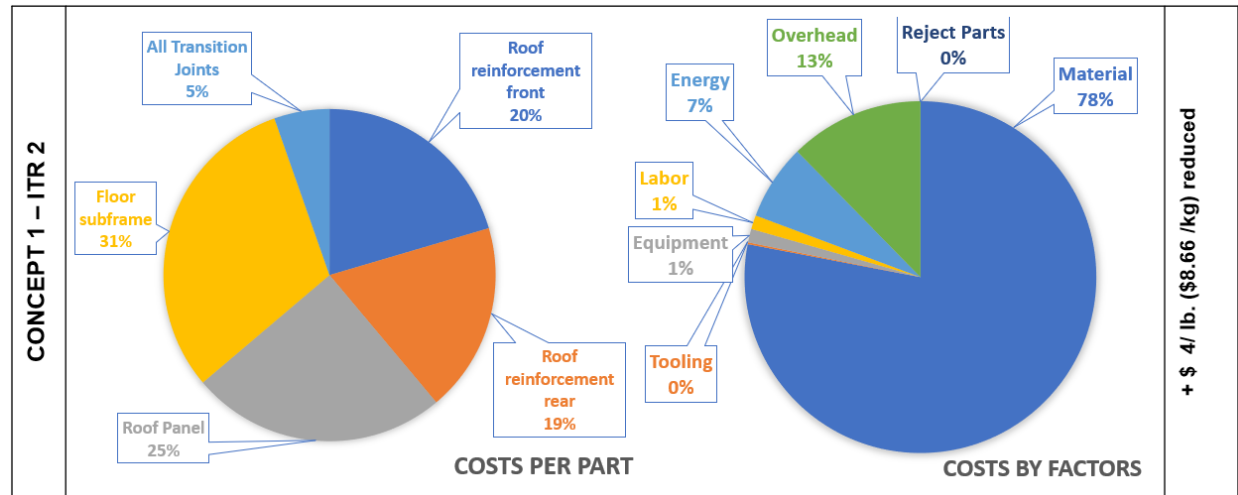


Figure 18: Cost model - concept 1, iteration 2 after optimization of composite components.

8. FUTURE WORK

Based on the free size optimization, zones of uniform thicknesses will be determined for all parts and further optimized. Currently, the optimization procedure focuses on static load cases. The design optimization procedure will be refined to include the dynamic cases. Further, the ply orientation and number will also be optimized. As it is observed that most regions in the optimization achieve the min thickness limits, GFRP and hybrid CF and GF composites are also being considered for further reduction in the cost. Composite manufacturing process parameters significantly affect the component's microstructure and, thus, the mechanical performance. Hence, coupled analyses, where microstructure obtained from process simulations is overlaid onto finite element mesh for mechanical performance assessment, are being investigated for HPRTM and WCM processes.

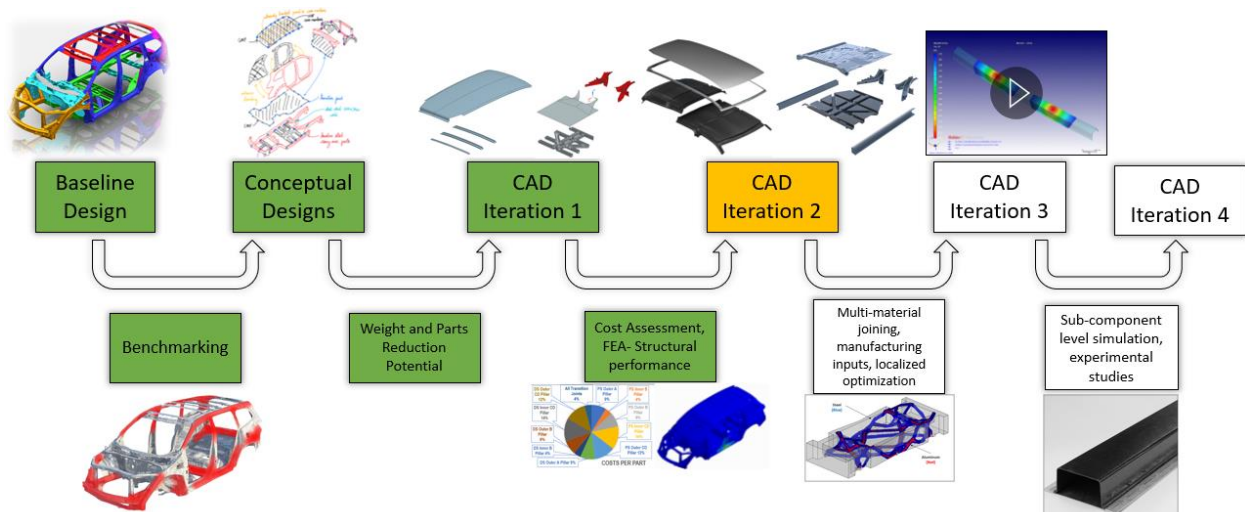


Figure 19: Future design studies and investigations.

Future work will target the implementation of the transition joint into the multi-material body simulations. A highly accurate yet computationally friendly model of the joint was developed by

segmenting the joint into a fiber-only, metal-only, and hybrid region. The fiber- and metal-only regions were defined using material cards from the literature, while the hybrid region was defined according to stress-strain analyses. This “Generalized” transition joint model was validated against a series of experimental tests, as seen in Figure 20. These results show that the generalized model provides a sufficiently accurate representation of the transition joint and can be passed directly into the multi-material simulations to represent the transition joint. Additional work is being completed to validate the accuracy of the transition joint, including compressive testing and implementation into a top-hat and double-hat structure, both common sub-components for automotive applications [2]. These analyses will be the first validation of the transition joint model at a component level while ensuring a minimal increase in the computational cost of the model.

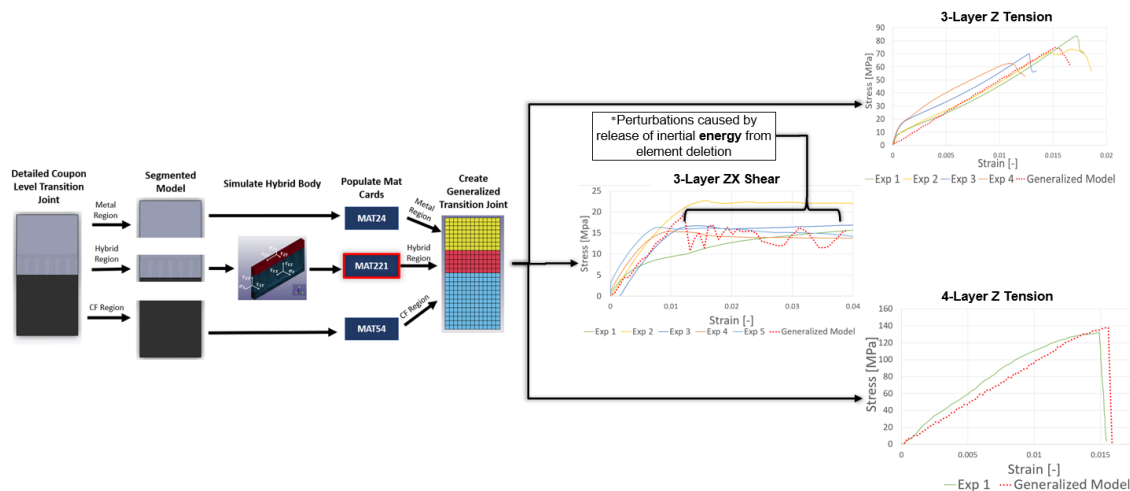


Figure 20: Framework for developing and validated generalized transition joint model to be used in multi-material simulations.

9. CONCLUSIONS

This study showcases the systems approach taken to conceptualize, design and optimize solutions for automotive lightweighting using a multi-material methodology while ensuring the cost and structural performance. Parts consolidation plays a key role in achieving cost-effective lightweighting as it leads to secondary cost savings through simplifying the assembly process and most of all, by eliminating multiple sheet-metal stamping tools, presses, and associated handling and joining equipment. This also helps offset FRP composite materials' higher material cost than conventional automotive steel grades. Conceptual redesign, followed by iterative design refinement of the concepts with inputs from successive design assessments regarding cost and lightweighting, have helped unlock greater scope for lightweighting possible through simple material substitution. However, material costs still play a dominant role in the cost-effectiveness of the designs, necessitating the need to extract additional structural functionality and performance from expensive composite materials. Optimization of these refined concepts helps achieve additional lightweighting while also reducing the amount of expensive composite materials used, allowing for much more cost-competitive designs.

Despite the developed designs being close to the cost objectives, the total lightweighting achieved by each standalone concept is insufficient to meet the lightweighting target of 72.5 kg, as illustrated in Figure 2. Thus, the two proposed concepts are being combined to achieve the required lightweighting target. Future efforts on the design and optimization front will be focused on developing this combined concept design to meet the cost targets, as illustrated in Figure 21.

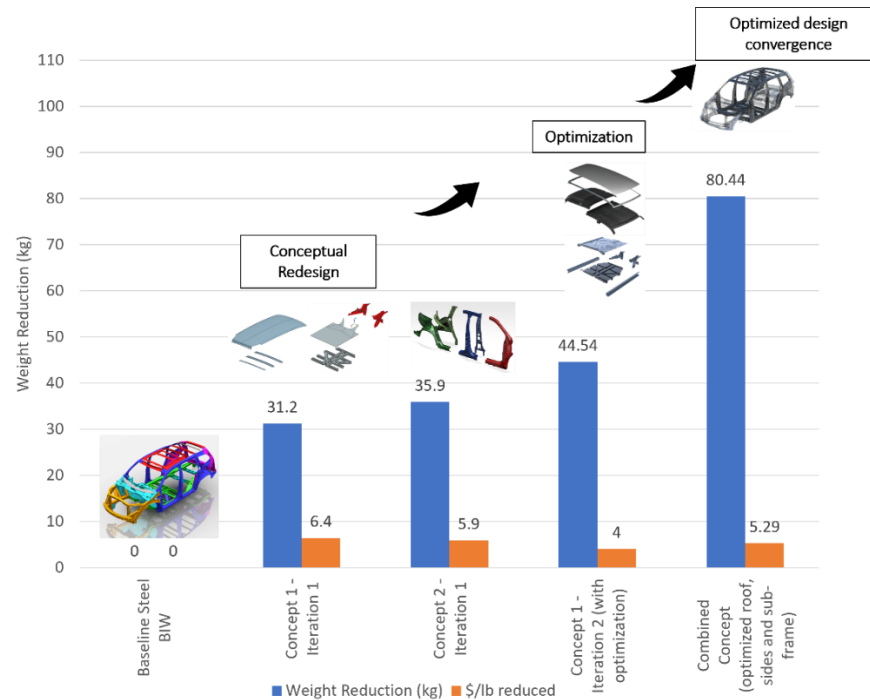


Figure 21: Mass and cost progression with development and optimization of multi-material BIW design.

10. ACKNOWLEDGEMENTS

The authors would like to acknowledge partial financial support from the Department of Energy, Project # DE-EE0009656 and industry partners including Siemens, Moldex3D, Westlake Epoxy, MSC Software (Hexagon), Zoltek and Carbon Conversions Inc. Marcelo J Dapino wishes to acknowledge the member organizations of the Smart Vehicle Concepts Center (www.SmartVehicleCenter.org), a Phase III National Science Foundation Industry–University Cooperative Research Center under Grant NSF IIP 1738723.

11. DISCLAIMER

Analysis and findings do not represent the designs or development methodology used by Honda for production vehicles.

12. APPENDIX

Table 4: CNC machining cost for HPRTM, WCM tools

CNC machining				
	Description	Amount (\$)	Comments	
Machine Costs	Machine Cost	\$ 350,000.00	purchase price of the machine	
	Machine insurance	\$ 35,000.00	insurance rate per year	10%
	Depreciation	\$26,250.00	per year depreciation (averaged rate)	8%
	Salvage Value	\$ 87,500.00	Value after 10 Years	
Total Machine Cost		\$ 1,750.00	Per Year	

Fixed Yearly Overheads	Administrative Costs	\$ 7,500.00	per year	
	Planned Maintenance Costs	\$ 17,500.00	fixed % per year of the machine cost	5%
	Labor Costs	\$ 21,840.00	per hour	\$ 30.00
			hours per year (52 weeks, 7 days a week, 8 hours a day, 50% uptime)	728
Variable Overheads	Unplanned maintenace Costs	\$ 35,000.00	fixed % per year of the machine cost	5 %
			expected frequency	2
	Electricity	\$ 11,793.60	Power rating (kWh)*hours per year*industrial electricity rate	15.00
				\$ 0.09
			hours per year (52 weeks, 7 days a week, 24 hours a day, 100% uptime)	8736
Yearly Consumables and spare parts	Carbide End mills	\$ 200.00	unit cost	\$ 50.00
			units required per year	4
	Collet Set	\$ 400.00	unit cost	100
			units required per year	4
	End Mill Holder	\$ 360.00	unit cost	90
			units required per year	4
	Ball Cutter	\$ 240.00	unit cost	60
			units required per year	4
	Coolant	\$ 1,080.00	unit cost	90
			units required per year	12
	Fixtures	\$ 1,000.00	unit cost	250
			units required per year	4
Total Yearly Cost of Operation		\$ 597,413.60	Per Year	
Hourly Machine Rate		\$ 68.39	\$/h	

Table 5: Costs per part for Concepts 1 and 2 (iteration 1)

Concept 1		Concept 2	
Part Name	Cost per part	Part Name	Cost per part
Roof Cross Members	\$41.09	PS Outer A Pillar	\$71.46
Roof Panel	\$271.82	PS Inner B Pillar	\$34.11
Floor Sub Frame	\$160.08	PS Outer B Pillar	\$69.29
Floor Panel	\$160.41	PS Inner CD Pillar	\$111.61
All Transition Joints	\$28.63	PS Outer CD Pillar	\$101.33
		DS Outer A Pillar	\$71.46
		DS Inner B Pillar	\$34.11
		DS Outer B Pillar	\$69.29
		DS Inner CD Pillar	\$111.61
		DS Outer CD Pillar	\$101.33
		All Transition Joints	\$33.32
TOTAL	\$662.04	TOTAL	\$808.91

Table 6: Cost of composite parts by factors for Concepts 1 and 2 (iteration 1)

Concept 1		Concept 2	
Factor	Cost of composite parts per BIW	Factor	Cost of composite parts per BIW
Material	\$562.66	Material	\$656.72
Tooling	\$1.10	Tooling	\$2.64
Equipment	\$3.24	Equipment	\$14.59
Labor	\$6.00	Labor	\$15.00

Energy	\$6.40	Energy	\$18.81
Overhead	\$82.61	Overhead	\$101.16
Reject Parts	\$0.0022	Reject Parts	\$0.0026
TOTAL	\$662.04	TOTAL	\$808.91

13. REFERENCES

- [1] S. A. Pradeep, R. K. Iyer, H. Kazan, and S. Pilla, "Automotive Applications of Plastics: Past, Present, and Future," *Applied Plastics Engineering Handbook: Processing, Materials, and Applications: Second Edition*, pp. 651–673, Jan. 2017, doi: 10.1016/B978-0-323-39040-8.00031-6.
- [2] C. Oberste, "Investigating the Relationship between Fiber Length, Volume Fraction, and Mechanical Properties of Fiber-Reinforced Plastics Lightweighting for the Masses™," 2019.
- [3] "Document Display | NEPIS | US EPA." <https://nepis.epa.gov/Exe/ZyPDF.cgi/P100Z3O4.PDF?Dockkey=P100Z3O4.PDF> (accessed Feb. 26, 2022).
- [4] "Plastics makers plot the future of the car." <https://cen.acs.org/articles/95/i45/Plastics-makers-plot-future-car.html> (accessed Feb. 26, 2022).
- [5] "2017-2025_CAFE-GHG_Supplemental_NOI07292011", Accessed: Feb. 27, 2022. [Online]. Available: https://www.nhtsa.gov/staticfiles/rulemaking/pdf/cale/2017-2025_CAFE-GHG_Supplemental_NOI07292011.pdf
- [6] A. M. Deshpande *et al.*, "Design and Development of a Multi-material, Cost-competitive, Lightweight Mid-size Sports Utility Vehicle's Body-in-White," in *CAMX 2022 | Anaheim, CA*, 2022. doi: 10.33599/nasampe/c.22.0148.
- [7] P. Malnati, "Composites as auto-body reinforcements," *Compositesworld*, 2021. <https://www.compositesworld.com/articles/composites-as-auto-body-reinforcements> (accessed May 13, 2022).
- [8] J. Starke, "CARBON COMPOSITES IN AUTOMOTIVE STRUCTURAL APPLICATIONS".
- [9] "First Body-in-White Made from Composites for a Chinese Electric Car", Accessed: Jun. 05, 2022. [Online]. Available: www.springerprofessional.com/automotive
- [10] J. Takahashi, "Strategies and Technological Challenges for Realizing Lightweight Mass Production Automobile by using Thermoplastic CFRP," 2011. Accessed: Jun. 27, 2022. [Online]. Available: <http://j-t.o.oo7.jp/publications/20110820ppt.pdf>
- [11] M. R. Bambach, "Fibre composite strengthening of thin steel passenger vehicle roof structures," 2013, doi: 10.1016/j.tws.2013.09.018.
- [12] "automotive structural adhesives." <https://www.sae.org/news/2019/08/automotive-structural-adhesives-overview> (accessed Jun. 19, 2023).
- [13] "Adhesives in Automotive Assembly | Adhesives & Sealants Industry." <https://www.adhesivesmag.com/articles/98072-adhesives-in-automotive-assembly> (accessed Jun. 19, 2023).
- [14] H. Guo, M. B. Gingerich, L. M. Headings, R. Hahnen, and M. J. Dapino, "Joining of carbon fiber and aluminum using ultrasonic additive manufacturing (UAM)," *Compos Struct*, vol. 208, pp. 180–188, Jan. 2019, doi: 10.1016/J.COMPSTRUCT.2018.10.004.
- [15] C. Fais, "Lightweight automotive design with HP-RTM," *Reinforced Plastics*, vol. 55, no. 5, pp. 29–31, Sep. 2011, doi: 10.1016/S0034-3617(11)70142-4.
- [16] "Dynamic Fluid Compression Molding A new process for composite mass-production," 2016.
- [17] A. Mittal *et al.*, "Designing a Production-Ready Ultra-Lightweight Carbon Fiber Reinforced Thermoplastic Composites Door," in *SAE Technical Papers*, SAE International, Apr. 2021. doi: 10.4271/2021-01-0365.
- [18] V. aditya Yerra, S. Aditya Pradeep, and S. Pilla, "A SYSTEMS APPROACH TO DEVELOP ULTRA LIGHTWEIGHT COMPOSITE DOOR USING FIBER REINFORCED THERMOPLASTICS," 2018, Accessed: Aug. 02, 2022. [Online]. Available: <https://www.researchgate.net/publication/332438363>
- [19] M. S. Sarfraz, H. Hong, and S. S. Kim, "Recent developments in the manufacturing technologies of composite components and their cost-effectiveness in the automotive industry: A review study," *Compos Struct*, vol. 266, Jun. 2021, doi: 10.1016/J.COMPSTRUCT.2021.113864.
- [20] H. Guo, M. B. Gingerich, L. M. Headings, R. Hahnen, and M. J. Dapino, "Experimental investigation of CFRP-AA structures joined by ultrasonic additive manufacturing (UAM) and resistance spot welding (RSW)," *Compos B Eng*, vol. 260, p. 110768, Jul. 2023, doi: 10.1016/J.COMPOSITESB.2023.110768.